1985, *18*, 995), loops, trains, and tails (*Ibid.* 1986, *19*, 2353), and stars (Croxton, C. A. submitted for publication in *Macromolecules*).
(7) Croxton, C. A. *J. Phys. A: Math. Gen.* 1986, *19*, 987.
(8) Croxton, C. A. *Phys. Lett. A* 1985, *111*, 453.
(9) Croxton, C. A. In *Fluid Interfacial Phenomena*; Croxton, C. A., Ed.; Wiley: Chichester and New York, 1986; Chapter 7, p 343 ff.
(10) Croxton, C. A. *Statistical Mechanics of the Liquid Surface*; Wiley: Chichester and New York, 1980.
(11) Pratt, L. R.; Chandler, D. *J. Chem. Phys.* 1977, *67*, 3683.
(12) Croxton, C. A. to be published in *Macromolecules*.
(13) Bishop, M.; Kalos, M. H.; Sokal, A. D. *J. Chem. Phys.* 1983, *79*, 3496.

Molecular Weights and Solution Properties of a Series of Side-Chain Liquid Crystalline Polymers with Ethylene Oxide Spacers

R. Duran*† and C. Strazielle

Institut Charles Sadron (CRM-EAHP), Strasbourg, Cedex 67083, France.
Received December 3, 1986

ABSTRACT: A homologous series of methacrylate side-chain liquid crystalline (LC) homopolymers and copolymers was studied in solution by several techniques. The molecular weight distributions and some hydrodynamic and thermodynamic parameters were calculated. A decrease in the dn/dc values of the copolymers compared to those of their corresponding homopolymers was attributed to a higher density in solution of the homopolymers presumably caused by biphenyl–biphenyl interaction. A large discrepancy was found between the molecular weights found by classical size exclusion chromatography and those found by direct methods. Also an odd–even effect as a function of spacer length was seen in the exponent of the viscosity law and the Flory χ value.

Introduction

Though much research has been done on side-chain liquid crystalline (LC) polymers in the solid state,[1,2] to date relatively little attention has been paid to the properties of these polymers in solution.[3,4] Knowledge of solution properties, however, can be helpful in several ways. First and most obviously, solution properties must be known to be sure of correct molecular weight determination by all but chemical methods. Often molecular weights are claimed by size exclusion chromatography (SEC) or viscosometric methods which have been calibrated with polymers having entirely different properties than LC polymers. Second, it is thought that knowledge of the hydrodynamic properties of side-chain LC polymers in solution can give valuable insights into their solid-state behavior. Third, studies of these types of polymers are inherently interesting insofar as they can lead to a better understanding of the solution state.

It was therefore interesting to compare the results obtained for a series of side-chain LC polymers studied by several techniques: SEC, light scattering coupled SEC (LS–SEC) and classical light scattering (LS) in solution. These techniques can also give complementary thermodynamic and hydrodynamic parameters which permit further understanding of these LC polymers in solution.

As part of a collaborative effort, we are interested in LC polymers with ethylene oxide spacers; the polymer synthesis, liquid crystalline properties, and structural characterization are reported elsewhere.[5–7] The polymers studied here consisted of two homologous series. The first was a series of homopolymers with a methacrylate backbone to which was attached an oligo(ethylene oxide) spacer with a methoxybiphenyl mesogenic group as shown below. The spacer length varied from zero, i.e., the methoxybiphenyl attached directly to the backbone, to four ethylene oxide units, i.e. a tetrakis(ethylene oxide) spacer. In the text, these polymers are referred to by the abbreviation PM- with a number indicating the length of the spacer. For example, PM-2 indicates the methacrylate homopolymer with a bis(ethylene oxide) spacer. A series of four random methacrylate copolymers was also studied. These copolymers contained two different length spacers in a 50% ratio. They are abbreviated by PM- with two numbers separated by a comma indicating the respective spacer lengths; for example, PM-2,3 indicates the methacrylate copolymer of monomers with a bis(ethylene oxide) and a tris(ethylene oxide) spacer, respectively.

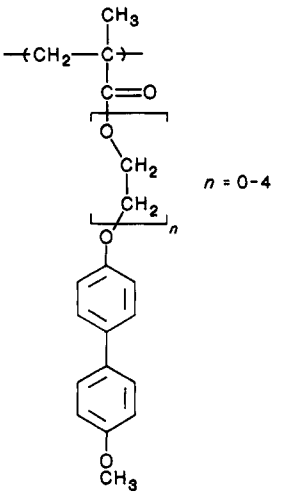

Experimental Section

(A) Samples. The series of methacrylate homopolymers and copolymers used in this study were synthesized in the laboratory of Ph. Gramain at the ICS, Strasbourg. Their synthesis and characterization has been described elsewhere.[6] THF and $CHCl_3$ used for the solutions were dried and distilled twice before use.

(B) Methods. (i) Light Scattering (LS). Weight-average molecular weights, M_w, were determined in THF or $CHCl_3$ solutions by a Fica 50 instrument. Measurements were made with

†Current address: Max Planck Institut fur Polymerforschung, D6500, Mainz, FRG.

0024-9297/87/2220-2853$01.50/0

Table I
Refractive Index Increments, dn/dc, at λ = 546 nm, Partial Specific Volumes of the Polymers, and Triad Tacticity Data

sample	dn/dc (mL/g) in THF	dn/dc (mL/g) in $CHCl_3$	$\bar{v}$ (mL/g) in THF	tacticity (% triads)[6] iso	hetero	syndio
PM-0	0.196[a]	0.163		20.1	34.4	45.1
PM-0,1	0.194			28.9	43.3	27.8
PM-1	0.212[b]	0.180		14.4	35.8	49.7
PM-1,2	0.188	0.153		9.3	34.8	55.7
PM-2	0.205	0.167	0.76_3	12.2	33.8	53.8
PM-2,3	0.170		0.77_5	9.4	33.4	57.1
PM-3	0.181	0.152	0.76_8	11.2	34.7	53.7
PM-3,4	0.153		0.81_2	10.6	34.1	55.3
PM-4	0.171	0.152	0.80_7	10.7	34.2	55.1

[a] Calculated from LS–SEC constants (see text). [b] Estimated (see text).

vertically polarized light of wavelength 546 nm at 25 ± 0.1 °C. The scattered intensity, $P(\theta)$, was measured at angles between 30 and 150 deg, and the results were analyzed by the classical method of Zimm. Before measurements, solutions were centrifuged at 15 000 rpm for 90 min to remove dust.

(ii) Size Exclusion Chromatography (SEC) and Light Scattering Coupled Size Exclusion Chromatography (LS–SEC). The SEC measurements were made on an apparatus consisting of two columns of 10-μm grain size and variable porosity, permitting separation in the mass range from 1×10^3 to 2×10^6 (in polystyrene equivalent mass). Instantaneous concentrations of the fractions separated by the columns were determined by a differential refractometer (Waters R401) and UV detection (Shimadzu SPD-2A). The columns were calibrated with a series of monodisperse PS standards in the molecular weight range from 1.5×10^3 to 1.4×10^6. For the LS–SEC measurements, a light-scattering cell of 80 μL volume was added between the concentration detectors at the exit of the column. The scattered intensity at an angle of 90 deg (valid for molecules of radius of gyration less than 40 nm) was measured by using a modified Fica 42000 instrument equipped with a He–Ne laser (λ = 632 nm). The mass of each fraction was then calculated from the measured scattered intensity and concentrations as has been described previously.[8]

(iii) Refractive Index Increments. Refractive index increment measurements were made with a Brice Phoenix differential refractometer at room temperature in THF or $CHCl_3$ solution.

(iv) Specific Volumes. Solution specific volumes were measured in a vibrating quartz cell described elsewhere.[9] The measurements were made at atmospheric pressure and thermostated to 0.01 °C. Calibrations were made with air and triple-distilled H_2O.

Results and Discussion

I. Refractive Index Increment and Partial Specific Volume. For accurate molecular weight determination by LS and LS–SEC, the refractive index increment in solution, dn/dc, must be known with precision. The refractive index increments used here were measured with a differential refractometer with less than 2% error. Care was taken to only make measurements on nonaggregated solutions that were well in solution. Values of dn/dc measured at 546 and 632 nm were equal within the error of the instrument; thus, only values at 546 nm are presented. Table I shows the dn/dc results measured in THF and $CHCl_3$ for the series. It should be noted that the first two methacrylate homopolymers, PM-0 and PM-1, showed very low solubility in THF; thus, direct measurement of dn/dc was impossible on the instrument used. For the PM-0 polymer, the dn/dc was calculated by using the LS–SEC calibration constants of PS and the PM-0 polymer.[10] For the PM-1 polymer, the dn/dc in THF was estimated from the dn/dc measured in $CHCl_3$, and the differences in dn/dc in THF and $CHCl_3$ were measured for each of the other polymers.

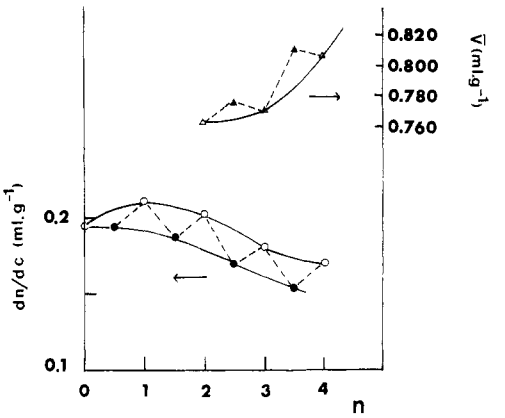

Figure 1. Refractive index increments, dn/dc, at λ = 546 nm (○, ●) in THF and partial specific volumes at 25 °C in THF (△, ▲). Unfilled and filled symbols represent homopolymers and copolymers, respectively. The dashed line is a visual aid to show the shift in the curves and has no physical significance.

Figure 1 shows the dn/dc values as a function of the spacer length obtained for the homopolymers and copolymers. The systematic shift in dn/dc for the copolymers to lower values than the homopolymers is noteworthy. Generally, dn/dc obeys the law of mixtures for copolymers,[11]

$$dn/dc_{cop} = x_a\nu_a + (1 - x_a)\nu_b \quad (1)$$

where ν_a and ν_b are the incremental components of the refractive index and x_a the fractional composition. For these copolymers, x_a is always close to 0.5 and thus eq 1 is not obeyed and the observed decrease in dn/dc is significant. To further understand this result, the relation of Gladstone and Dale is recalled:

$$dn/dc = R - (n_0 - 1)\bar{v} \quad (2)$$

where R is the solid-state refractivity of the polymer ($R = (n_P - 1)/d$, n_P is the polymer refractive index, d is the polymer density), $\bar{v}$ the partial specific volume of the polymer, and n_0 the refractive index of the solvent. This relation, though semiempirical, describes well dn/dc.[12,13]

For a copolymer obeying the law of additivity, one would thus expect

$$R = (R_a + R_b)/2 \quad \text{and} \quad \bar{v} = (\bar{v}_a + \bar{v}_b)/2 \quad (3)$$

Assuming that the refractivities do not deviate far from additivity, a significant change in the partial specific volumes of the polymers would be expected. These values were obtained by measuring specific volumes for a series of solutions of different concentrations, by

$$\bar{v} = v_0 + (v - v_0)/w \quad \text{as} \quad w \to 0 \quad (4)$$

where v_0 and v are the specific volumes of the solvent and solution, respectively, and w is the concentration expressed in g/g.

The obtained values are shown in Table I and plotted in Figure 1. The copolymers are seen to have partial specific volumes significantly higher than those of the homopolymers. Though the change in dn/dc cannot be quantitatively explained by the change in the specific volume term of eq 2 alone, the nonadditivity seen in the dn/dc values seems in part to come from a densification of the homopolymers in solution relative to the copolymers. This effect is plausible when one considers that in the case of random copolymers of different spacer lengths, much less biphenyl–biphenyl interaction is expected than in the case of homopolymers.

II. Molecular Weights and Polydispersity. Of the different molecular parameters determined by LS, LS–

Table II
Molecular Weights and Polydispersities for Homopolymers

sample	LS M_w THF	LS M_w $CHCl_3$	LS–SEC (THF) M_n	LS–SEC (THF) M_w	SEC (THF) M_w*	SEC (THF) M_w*/M_n*
PM-0 RP33			6000	22700	9900	2.5
PM-0 RP38			3000	5300	3200	1.6
PM-0 RP27		87400[a]				
		26000[b]				
PM-1 RP23		34700				
PM-2 RP1	67300	74500	22800	65000	41350	2.8_4
PM-3 RP6	37600	49600	16700	45900	27200	2.6
PM-4 RP49	200000	195000	64800	183000	99800	2.7_3
PM-4 RP51			6500	17600	10500	2.7_0
PM-4 RP50			16000	160000		

[a] Determined at $\theta = 0°$. [b] Determined at $\theta = 90°$ (see text). [c] Bimodal distribution (see Figure 5). The RP is an arbitrary reference of the specific sample measured with no physical significance but allows for comparison of the same samples in other publications.

Table III
Molecular Weights and Polydispersities for Copolymers

sample	LS M_w (THF)	LS–SEC (THF) M_n	LS–SEC (THF) M_w	SEC (THF) M_w*	SEC (THF) M_w*/M_n*
PM-0,1 RP64	34500	12400	39300	18000	2.6_6
PM-1,2 RP25	49800	21400	49200	25300	2.3_0
		20600	48900[a]	26300	2.2_6
PM-2,3 RP28	67800	24000	67600	33900	2.5_8
PM-3,4 RP53	36000	14100	34400	19600	2.0

[a] Data from a repeat determination.

SEC, and SEC, molecular weights and polydispersity are the most often discussed. Here M_w determined by direct classical LS; M_w, M_n, and $I = M_w/M_n$ determined by LS–SEC; and M_w*, M_n*, and I* = M_w*/M_n* (the PS equivalent masses) determined by classical SEC will be discussed.

The molecular weight results for the homopolymer and copolymer series are summarized in Tables II and III, respectively. From these results, several comments can be made.

The molecular weights measured by LS and LS–SEC for the copolymers (Table III) and homopolymers with spacer lengths of two or greater than two ethylene units (Table II) are in excellent agreement. The homopolymers with shorter spacers, however, show much lower (PM-0) or virtually no (PM-1) solubility in THF, making their analysis much more difficult. Figure 2 shows the LS–SEC curve for a PM-0 polymer. Even at the low (0.5 g/L) polymer concentrations used, the huge ΔI peak in the high mass elution volume region and correspondingly no ΔC peak indicate the formation of aggregates in solution. This is also indicated by the strong curvature seen in the LS plot in $CHCl_3$ shown in Figure 3. The mass calculated from the small-angle region is strongly overestimated (87400), while the mass from the large-angle region is 26000 (see Table II). The THF solutions were, however, made aggregate-free by heating followed by cooling, although upon aging new aggregates formed. The PM-0 polymer easily formed stable thermoreversible gels on cooling from hot dilute chlorobenzene solution, indicating aggregation behavior in this solvent as well.

The PM-1 polymer showed negligible solubility in THF at room temperature. The polymer was slightly soluble on heating, though on cooling new aggregates formed immediately. The PM-1 polymer in $CHCl_3$ showed classical Zimm plots with little dissymmetry.

The PM-2, PM-3, and PM-4 homopolymers showed good solubility in both THF and $CHCl_3$ and no evidence of aggregates by LS–SEC nor dissymmetry in LS.

Figure 4 shows the Zimm plot and LS–SEC curves for the PM-4 (RP49) polymer. The curves in Figure 4b represent the concentration (ΔC) and scattered intensity (ΔI)

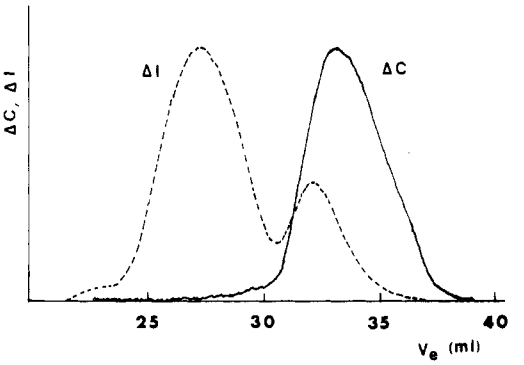

Figure 2. ΔI (LS) and ΔC (refractometry) chromatograms from LS–SEC analysis of PM-0 (RP33) aggregated sample.

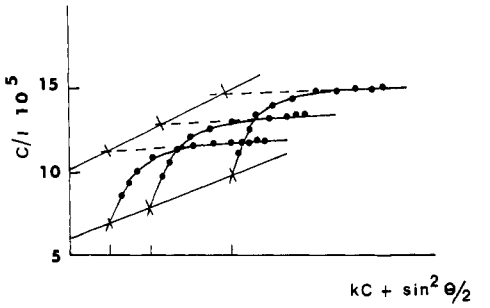

Figure 3. Zimm plot of an aggregated PM-0 (RP27) sample in $CHCl_3$.

as a function of the elution volume. The smooth distribution curves in Figure 4b and lack of curvature in Figure 4a indicate the absence of aggregates.

The occurrence of aggregates in side-chain LC polymers has been proposed by Springer and Weigelt,[3,4] though little direct evidence was presented. The above authors suggested that the backbone tacticity may influence the aggregation process. In these polymers, it is thought that biphenyl–biphenyl interactions play the dominant role. This is suggested by the fact that all the copolymers are well soluble even though the PM-0,1 copolymer has about 30% isotactic triads.[6] Furthermore, as is shown in Table I, the triad tacticities of the other polymers and copolymers were very similar, though the solubilities varied. The role of the biphenyls is also supported by the densification of the homopolymers, where more biphenyl–biphenyl contact is permitted, compared to the copolymers in solution.

The analysis of the results by SEC was made from the relation $V_e = \alpha + \beta \log M$, with α and β determined by calibration with PS standards. The PS equivalent masses, M_w* and M_n*, obtained were systematically lower than those obtained by light-scattering methods. The error thus obtained by SEC M_w measurements alone was about 50%

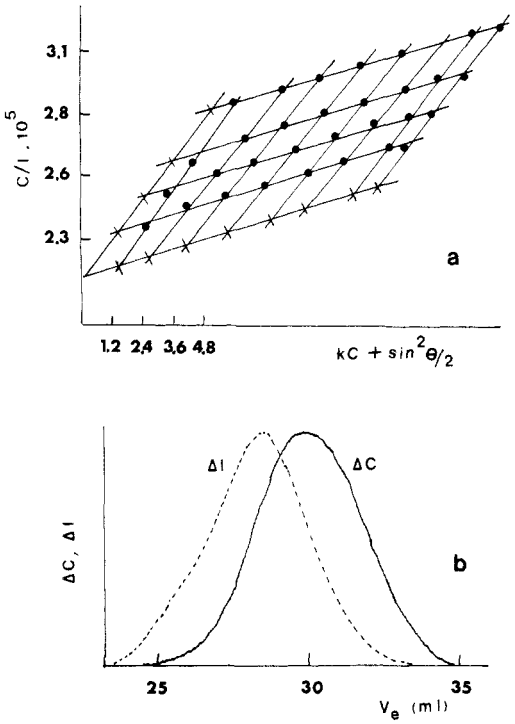

Figure 4. Molecular weight determination of PM-4 (RP49) in THF: (a) Zimm plot from classical light scattering, (b) ΔC (refractometry) and ΔI (LS) chromatograms from LS–SEC.

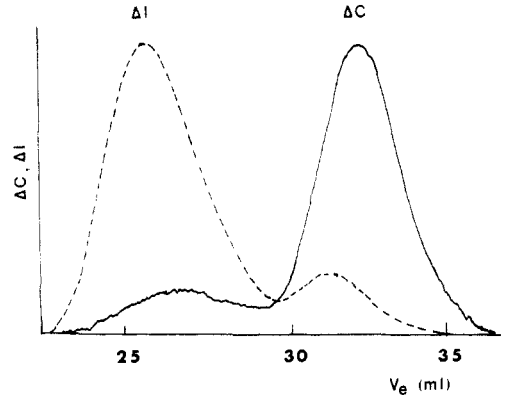

Figure 5. Bimodal distribution for PM-4 (RP20) obtained from LS–SEC analysis in THF.

of the LS values. This large error is understandable when one considers that the SEC separation process is not governed by the mass but by the hydrodynamic volume, that is, the product $(\eta)_i M_i$ of the fraction,[14] ($(\eta)_i$ is the intrinsic viscosity of a fraction of mass (M_i) associated with an elution volume (V_{e_i})). This point will be discussed in more detail in part III below.

The molecular weight distributions measured by LS–SEC were generally normal for free-radical polymerization with polydispersities from 2.0 to 2.8. A typical distribution curve is shown on Figure 6 for a PM-4 (RP49) polymer. In one case, however, a bimodal distribution was observed. This was observed for a PM-4 (RP20) polymer by LS–SEC and is shown on Figure 5. The two peaks seen in both of the ΔC and ΔI curves indicate that this is a bimodal distribution and not the formation of aggregates. The peaks are at masses of 570 000 and 19 300, respectively. Analysis of the two peaks together shown in Table II gives M_n 16 000, M_w 160 000, and a very high polydispersity index of 10.

Finally, it was noted that all the second virial coefficients, A_2, determined by LS in THF were of the order of

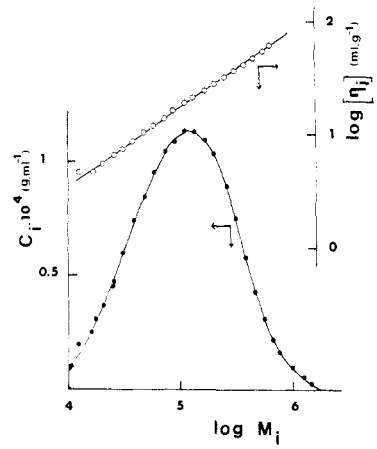

Figure 6. Molecular weight distribution and viscosity law for PM-4 (RP49) in THF.

2×10^{-4} to 4×10^{-4} mol·mL·g^{-2}, indicating that THF is a good solvent for these polymers with n greater than or equal to 2.

III. Hydrodynamic Properties: Law of Viscosity. The LS–SEC technique can be used to determine the law of viscosity:

$$(\eta) = KM^a \tag{5}$$

This assumes that the universal calibration[14] is valid. As this has been verified in the case of PMMA,[10] it was thought to be reasonable to study these polymers as well. Then one can state for a given fraction, V_{e_i}, the equality of the hydrodynamic volumes:

$$(\eta)_i M_i = (\eta)_{ps} M_{PS} \tag{6}$$

As a consequence, one finds

$$(\eta)_i = (K_{PS} M_{PS}^{(1+a_{PS})})/M_i \tag{7}$$

where K_{PS} and a_{PS} are the parameters of the power law in THF for the PS standards used to calibrate chromatographic columns: $K_{PS} = 14 \times 10^{-3}$ and $a_{PS} = 0.7$ for (η) expressed in mL/g,[15] M_{PS} is the PS equivalent mass found from the calibration $V_e = \alpha + \beta \log M$, and M_i is the mass from the volume fraction, V_i, determined by LS–SEC. This technique of calculating the intrinsic viscosity eliminates the need for a series of monodisperse samples in determining viscosity law parameters. The universal calibration, however, must be valid with the sample studied, a reasonable assumption in this case. The dn/dc values must also be known over the molecular weight range studied; here, dn/dc values measured for small and large molecular weights of the PM-4 polymer (samples RP51 and RP49 from Table II) were identical, so dn/dc was assumed to be a constant over the M_w range examined.

Figure 6 shows the viscosity law determined for a PM-4 (RP49) polymer in the domain of mass between 8000 and 600 000 and the corresponding distribution curve. The viscosity law coefficients, K and a, for the polymers soluble in THF as well as a PMMA sample with about 60% syndiotactic triads are shown in Table IV. Because of the high masses, m, of the monomers (more than 400 for PM-4), it was interesting to reason in terms of degree of polymerization, n_w, as well. The viscosity law was established as a function of the degree of polymerization by

$$(\eta) = K' n_w^a \quad \text{with} \quad K' = Km^a \tag{8}$$

These results are also shown on Table IV. In Figure 7, the variations in the parameter K' (Figure 7a) and the exponent a (Figure 7b) are plotted. The preexponential factor,

Table IV
Viscosity Law Parameters in THF from Analysis in Terms of Mass and in Terms of Degree of Polymerization

	$(\eta) = KM^a$		$(\eta) = K'n_w^a$	
sample	10^3K	a	$10^2K'$	a
PMMA[10]	12.8	0.69	30.6	0.69
PM-2 RP1	7.35	0.69_5	44.3	0.69_4
PM-3 RP6	13.8	0.62_8	59.4	0.62_8
PM-4 RP49	6.4	0.68_5	81	0.68_7
PM-0,1 RP64	12.36	0.57_5	32.2	0.57_5
PM-1,2 RP25	10.0	0.63_4	39.7	0.62_7
PM-2,3 RP28	9.25	0.63_5	40.5	0.63_4
PM-3,4 RP53	18.7	0.59	65.3	0.59

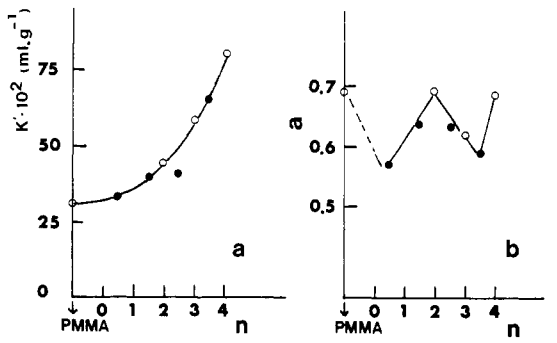

Figure 7. Variation of the viscosity law parameters K' and a versus n for homopolymer (○) and copolymers (●) in THF. Spacer length, n, expressed in number of ethylene oxide units.

K', related to the molecular dimensions, is seen to vary regularly with the number of ethylene oxide spacer units, n; it increases with longer spacers. The exponent, a, however, shows very unusual behavior. The a values for the PM-2 and PM-4 polymers are higher than the others and approach the 0.69 value observed for PMMA. In fact, this behavior resembles an odd–even hydrodynamic effect, though studies on longer spacer lengths would be necessary for confirmation.

IV. Unperturbed Dimensions and Interaction Parameters. To look at the effect of excluded volume and thus the expansion of the molecule in THF as a function of the spacer length, the unperturbed chain dimensions were calculated. The Stockmayer–Fixman[16] equation was used, assuming validity for this type of molecule:

$$(\eta)/M^{1/2} = K + 0.51B\varphi_0M^{1/2} \quad \text{with} \quad K = \varphi_0(\bar{r}_0^2/M)^{3/2} \tag{9}$$

where $\bar{r}_0^2$ is the mean square end-to-end distance, φ_0 is the Flory constant ($\varphi_0 = 2.7 \times 10^{23}$), and the intrinsic viscosity, (η), is expressed in mL/g. The parameter B can be related to the Flory interaction parameter, χ, by

$$B = 2\bar{v}_2/V_1N_a(1/2 - \chi) \tag{10}$$

where N_a is avogrado's number, v_2 is the polymer partial specific volume, and V_1 is the elemental volume of a Flory lattice unit, generally equated with the molar volume of the solvent. The statistical element length, b, can also be determined from the unperturbed dimension K by

$$b = (\bar{r}_0^2/M)^{1/2}m^{1/2} = (K/\varphi_0)^{1/3}m^{1/2} \tag{11}$$

where m is the mass of a monomer repeat unit. Considering the results in terms of the degree of polymerization rather than the mass, one obtains

$$(\eta)/n_w^{1/2} = K' + 0.51\varphi_0B'n_w^{1/2} \quad \text{with} \quad K' = Km^{1/2} \quad \text{and} \quad B' = Bm \tag{12}$$

To better compare the backbone dimensions as a function of the spacer length, the results were normalized to PMMA[10] as a reference by

$$(\bar{r}_0^2)_{PM\text{-}n}{}^{3/2}/(\bar{r}_0^2)_{PMMA}{}^{3/2} = (Km^{3/2})_{PM\text{-}n}/(Km^{3/2})_{PMMA} \tag{13}$$

The ratio $(\bar{r}_0^2)_{PM\text{-}n}{}^{1/2}/(\bar{r}_0^2)_{PMMA}{}^{1/2}$ then represents the ratio of the mean square end-to-end distances of the PM-n polymer compared to PMMA, both at a normalized degree of polymerization. One then has an idea of the chain rigidity relative to PMMA as a function of spacer length. The values are presented in Table V and indicate that the chains become increasingly rigid as the spacer length increases.

Table V
Unperturbed Dimensions and Interaction Parameters for Homopolymers and Copolymers in THF

sample	10^2K (mL/g)	b (Å)	$(\bar{r}_0^2)_{PM\text{-}n}{}^{1/2}/(\bar{r}_0^2)_{PMMA}{}^{1/2}$	$10^{28}B$ (mL/g²)	χ
PMMA	6.35	6.29	1.0	11.2	0.45_5
PM-0,1	2.60	7.96	1.26	0.72	0.49_2
PM-1,2	3.62	9.53	1.49	1.9	0.47_5
PM-2	4.82	10.80	1.72	4.87	0.43_2
PM-2,3	3.85	10.40	1.64	1.96	0.47_0
PM-3	4.80	11.50	1.82	2.69	0.45_7
PM-3,4	4.48	11.50	1.82	1.69	0.47_1
PM-4	3.84	11.20	1.78	3.50	0.43_9

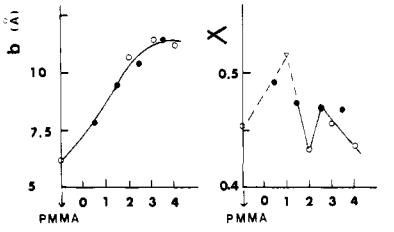

Figure 8. Variation of the statistical element length, b, and interaction parameter, χ, versus spacer length, n, for homopolymers (○) and copolymers (●) in THF. (▽) = χ value estimated for PM-1, estimated greater than 0.5 due to the very low solubility of this polymer.

The Stockmayer–Fixman relations were determined for the viscosity law in the mass range from 40 000 to 500 000. Table V shows the different parameters calculated for the series: K, the unperturbed chain dimensions; b, the statistic element length; and χ, the Flory interaction parameter. It should be noted that in calculating χ values from B, the Flory lattice volume, V_1, was normalized to PMMA in a manner similar to the K results above. Figure 8 shows the b values (Figure 8a) and the χ values (Figure 8b) plotted as a function of the spacer length. The b values increase, reaching a maximum for about three ethylene oxide units; this also indicates a rigidification of the chain as the spacer length increases. Furthermore, the χ values, like the exponent a from the viscosity law, seem to show an odd–even effect.

Conclusions

The systematic study of a series of LC homopolymers and copolymers by SEC, LS–SEC, and LS led to several conclusions.

A decrease in the refractive index increment was observed for the copolymers as compared to the homopolymers. This was attributed to a difference in the specific volumes of the polymers measured in solution, the homopolymers being denser, presumably due to biphenyl–biphenyl interactions.

A large discrepancy was observed in the molecular weights measured by the classical SEC technique calibrated with PS compared to direct measurement. It was

shown, however, that the direct measurement techniques of LS or LS–SEC yield precise, reproducible results.

A strong tendency toward formation of aggregates in solution was observed in the homopolymers with short spacers. This was not observed in the copolymers of similar spacer lengths, indicating a role of biphenyl–biphenyl interactions in this phenomenon as well.

An odd–even effect was observed in the measured exponent of the viscosity law as a function of the spacer length. This effect was also observed in the Flory χ values as a function of the spacer length.

The calculated end-to-end distances of the homopolymers and copolymers increased regularly with increasing spacer length, all being substantially greater than that of PMMA. This indicates that these polymers in solution are stiffer than PMMA and that the stiffness increases as the spacer length increases.

Acknowledgment. Dr. A. Skoulios and Dr. Ph. Gramain are gratefully acknowledged for advice which proved helpful in this work. J. Francois, D. Sarazin, and J. LeMoigne are thanked for the use of the specific volume apparatus. M. Mottin is thanked for help in running samples. R. D. would like to thank the French Scientific Mission for a Lavoisier Scholarship provided during the course of this work.

Registry No. PM-0, 103138-42-7; PM-0,1, 109976-74-1; PM-1, 68317-18-0; PM-1,2, 109976-75-2; PM-2, 103138-44-9; PM-2,3, 109976-76-3; PM-3, 103138-45-0; PM-3,4, 109976-78-5; PM-4, 109976-79-6.

References and Notes

(1) *Polymeric Liquid Crystals*; Blumstein, A., Ed.; Plenum: New York, 1985.
(2) *Recent Advances in Liquid Crystalline Polymers*; Chapoy, L. L., *Ed.*; Elsevier: Essex, 1985.
(3) Springer, J.; Weigelt, F. *Makromol. Chem.* **1983**, *184*, 1489.
(4) Springer, J.; Weigelt, F. *Makromol. Chem.* **1983**, *184*, 2635.
(5) Duran, R.; Gramain, Ph.; Guillon, D.; Skoulios, A. *Mol. Cryst. Liq. Cryst. Lett.* **1986**, *3*, 23.
(6) Duran, R.; Gramain, Ph. *Makromol. Chem.*, in press.
(7) Duran, R.; Guillon, D.; Skoulios, A. *Makromol. Chem. Rapid Commun.*, in press.
(8) Beltzung, L.; Strazielle, C. *Makromol. Chem.* **1984**, *185*, 1145.
(9) Sarazin, D.; LeMoigne, J.; Francois, J. *J. Appl. Polym. Sci.* **1978**, *22*, 1377.
(10) Beltzung, L.; Strazielle, C. *Makromol. Chem.* **1984**, *185*, 1155.
(11) Benoit, H.; Froelich, D. In *Light Scattering From Polymer Solutions*; Huglin, M. B., Ed.; Academic: London, 1973; Chapter 11.
(12) Bodmann, O. *Makromol. Chem.* **1969**, *122*, 209.
(13) Herz, M.; Strazielle, C. *Eur. Polym. J.* **1973**, *9*, 543.
(14) Grubisic, Z.; Rempp, P.; Benoit, H. *J. Polym. Sci. B* **1967**, *5*, 753.
(15) Strazielle, C.; Herz, J. *Eur. Polym. J.* **1977**, *13*, 223.
(16) Stockmayer, W. H.; Fixman, M. *J. Polym. Sci. C* **1963**, *1*, 136.

Electric Field Induced Light Scattering from Polar Polymers

Garo Khanarian* and Richard S. Stein

Polymer Research Institute, University of Massachusetts, Amherst, Massachusetts 01003.
Received January 15, 1987

ABSTRACT: A theory is presented for light scattering from a flexible polar polymer chain, in the presence of an electric field (EFLS). It is shown that the change in light scattering due to the applied electric field arises from two effects. First, the electric field deforms the polymer because the more polar configurations are energetically more favorable in the presence of the electric field. This fluctuation term is zero for rigid polymers. Second, the polymer orients in the field. It is also shown that the fluctuation and orientation terms can be separated by performing two experiments, where the applied field is normal and parallel, respectively, to the scattering vector. The general expressions that are derived in this paper for EFLS cannot be evaluated easily, for any polymer. However, in the small-angle scattering regime, the expressions for EFLS simplify so that they can be evaluated in the rotational isomeric state (RIS) scheme. EFLS promises to be a useful tool for characterizing semiflexible polymers and also complements other techniques (end-to-end distance, dipole moments, Kerr effect) for the characterization of polymers.

Introduction

The characterization of polymers by light scattering is a well-proven method from which we derive the structure factor, molecular weight, and solution second virial coefficient.[1] A closely related technique, electric field induced light scattering (EFLS),[2] has received less attention but is also potentially useful for polymer characterization. In the case of EFLS, we observe the change in light scattering intensity when a strong electric field E is applied across a medium. In the absence of an electric field we observe the isotropically averaged structure factor, which arises from the phase differences between different parts of a macromolecule. In the presence of a strong electric field, two additional effects occur; first, the polymer is oriented because of the interaction of the dipole moment with the electric field; second, in the case of flexible polymers, the shape is distorted by the electric field because the more polar conformations are energetically preferred. Thus, from an EFLS experiment, we can learn about polymer conformation and flexibility, and dipolar interactions with electrical fields.

EFLS is similar to two other nonlinear dielectric experiments; namely, the Kerr effect[3] and nonlinear dielectric effect (NLDE), or dielectric saturation.[4] The Kerr effect is the forward scattering of light in an electrical field which results in a change of refractive indices parallel and perpendicular to the applied field and gives information about polarizability, anisotropy, dipolar interactions, and polymer conformation. The NLDE is the change of the dielectric constant in a strong electrical field and gives information about polymer flexibility, conformation, and dipolar interaction.

Wippler, Benoit,[5,6] and, more recently, Jennings[2] have experimentally and theoretically studied EFLS and have

*Address correspondence to this author at Hoechst-Celanese Corporation, Summit, NJ 07901.

0024-9297/87/2220-2858$01.50/0